DALTON
FULL PAPER

Syntheses, structures and electrochemistry of copper(II) salicylaldehyde/tris(3-phenylpyrazolyl)borate complexes as models for the radical copper oxidases

Malcolm A. Halcrow,*[a] Li Mei Lindy Chia,[b] Xiaoming Liu,[c] Eric J. L. McInnes,[d] Lesley J. Yellowlees,[c] Frank E. Mabbs,[d] Ian J. Scowen,[e,f] Mary McPartlin[e] and John E. Davies[b]

[a] *School of Chemistry, University of Leeds, Woodhouse Lane, Leeds, UK LS2 9JT. E-mail: M.A.Halcrow@chem.leeds.ac.uk*
[b] *Department of Chemistry, University of Cambridge, Lensfield Road, Cambridge, UK CB2 1EW*
[c] *Department of Chemistry, The University of Edinburgh, West Mains Road, Edinburgh, UK EH9 3JJ*
[d] *EPSRC CW EPR Service Centre, Department of Chemistry, University of Manchester, Oxford Road, Manchester, UK M13 9PL*
[e] *School of Applied Chemistry, University of North London, 166–220 Holloway Road, London, UK N7 8DB*
[f] *Department of Chemistry and Chemical Technology, University of Bradford, Bradford, UK BD7 1DP*

Received 27th January 1999, Accepted 7th April 1999

2-Hydroxy-5-methyl-3-methylsulfanylbenzaldehyde (HL^2) and 2-hydroxy-5-methyl-3-methylselanylbenzaldehyde (HL^3) have been synthesized from 2-hydroxy-5-methylbenzaldehyde (HL^1), as have Schiff bases HL^4R and HL^5R (R = Me or Ph) derived from RNH_2 and HL^1 or HL^2 respectively. The complexes [Cu(L)(Tp^{Ph})] ([L]$^-$ = $[L^1]^-$, **1**; $[L^2]^-$, **2**; $[L^3]^-$, **3**; $[L^4Me]^-$, **4**; or $[L^4Ph]^-$, **5**) have been prepared. Single crystal structure determinations of **1**, **2**, **4** and **5** show copper(II) centres with square pyramidal [CuN_3O_2] (**1**, **2**) or [CuN_4O] (**4**, **5**) co-ordination spheres; for **4** and **5** the basal plane of the complex is twisted by 20–25° because of the steric properties of the Schiff base Me or Ph substituent. The UV/vis and EPR spectra of **1**–**5** in CH_2Cl_2 show the presence of tetragonal copper(II) centres. Cyclic voltammograms of **1**–**5** and the uncomplexed phenols in CH_2Cl_2–0.5 M $Bu^n_4NPF_6$ exhibit an irreversible or (for **2**) reversible 1-electron oxidation to a phenoxyl radical. The oxidation potentials of HL^2 and HL^3, and of **2** and **3**, are barely distinguishable. However, the irreversibility of this process for **3** compared to that of **2** suggests that a selenoether substituent kinetically stabilises the phenoxyl unpaired spin less efficiently than a thioether one; this is borne out by EHMO calculations on $L^{1\bullet}$–$L^{3\bullet}$. Spectroelectrochemical characterisation of $[\mathbf{2}]^+$, whose UV/vis/NIR spectrum is very similar to that of galactose oxidase, confirms its formulation as the antiferromagnetically coupled species [$Cu^{II}(L^{2\bullet})(Tp^{Ph})$]$^+$.

Introduction

The prototypical radical copper oxidase is galactose oxidase ('GOase'), an enzyme from wood-rot fungi that catalyses the oxidation of primary alcohols to aldehydes by molecular oxygen, eqn. (1).[1,2] Glyoxal oxidase, another fungal enzyme, catalyses the oxidation of aldehydes by O_2, eqn. (2), and has also been assigned to this class of enzyme on the basis of its spectroscopic properties.[3]

$$RCH_2OH + O_2 \longrightarrow RCHO + H_2O_2 \qquad (1)$$

$$RCHO + O_2 + H_2O \longrightarrow RCO_2H + H_2O_2 \qquad (2)$$

The single crystal structure of GOase shows a square-pyramidal [$Cu(His)_2(Tyr)_2(OH_2)$] centre with an apical phenoxide donor (Fig. 1).[4,5] Interestingly, the basal tyrosinate ligand has both been chemically modified by attack of a cysteine thiolate donor at the phenyl ring to form an *ortho*-thioether linkage, and is involved in a π-stacking interaction with a neighbouring tryptophan indole ring, whose function is unknown but which is essential for catalysis.[5] This chemically modified phenoxide ligand is readily oxidised to a very long-lived radical,[6] whose oxidation potential in the holoenzyme is only +0.40 V *vs.* NHE (compared to +0.9 V for a 'normal' tyrosine side-chain).[7] This phenoxyl radical acts as a H atom acceptor during the GOase oxidation reaction, eqn. (3), thus

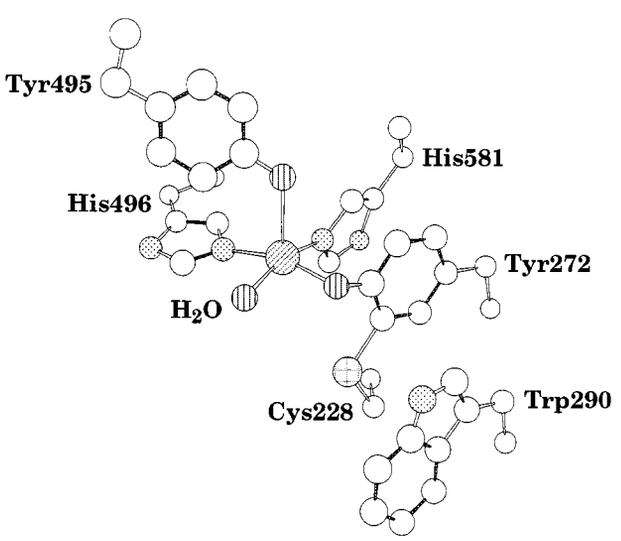

Fig. 1 Structure of the galactose oxidase copper site.

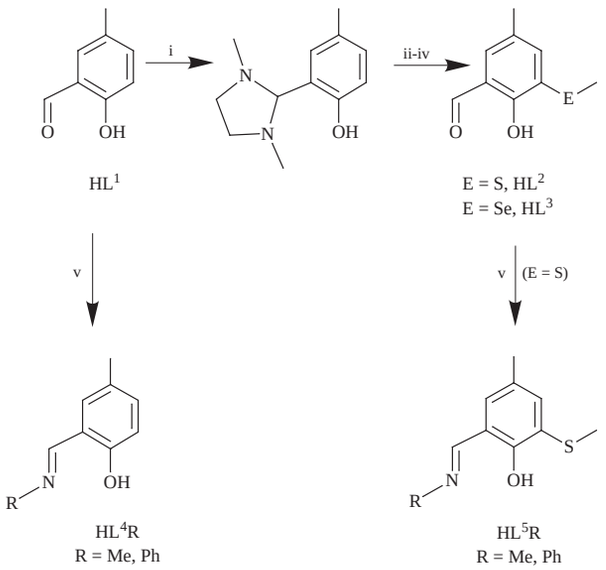

Scheme 1 (i) DMEDA, EtOH, $MgSO_4$, RT, 16 h; (ii) 4 equivalents Bu″Li/TMEDA, Et_2O, −78 °C to RT, 6 h; (iii) MeEEMe (E = S or Se), RT, 16 h; (iv) 2 M HCl, RT, 10 min; (v) RNH_2, MeOH.

allowing the mononuclear copper(II) site to effect a 2-electron oxidation reaction.

$$Cu^{II}/Tyr\cdot + RCH_2OH \longrightarrow Cu^{I}/Tyr^{-} + RCHO + 2H^{+} \quad (3)$$

The oxidised, active enzyme exhibits, in addition to lower wavelength peaks, an unusual intense vis/NIR envelope between 600 and 1 200 nm with ε_{max} = 3 200 M^{-1} cm^{-1}, which contains at least nine distinct electronic transitions.[1] During the past few years several model compounds for the GOase non-innocent tyrosinate moiety[8] and copper centre[9–18] have been described. However, to date no model system has successfully reproduced the electronic spectrum of active GOase. We have recently communicated the complex [Cu(L^2)(Tp^{Ph})] [Tp^{Ph} = hydridotris(3-phenylpyrazolyl)borate], whose 1-electron oxidation product represents the first example of a copper(II) phenoxyl species bearing an *ortho*-thioether side chain. Interestingly, this complex does exhibit a UV/vis/NIR spectrum closely resembling that of the oxidised enzyme.[19] We now present a full account of the synthesis, structural characterisation and electrochemistry of this and related compounds. In particular, we discuss the properties of a selenoether-substituted analogue of the above complex, which is intended to predict the effects of mutation of Cys-228 of GOase, which forms the cross-link to the basal tyrosinate ligand (Fig. 1), to a selenocysteine residue in the GOase active site.

Results and discussion

Syntheses and spectroscopy of the ligands and complexes

Our choice of ligands was governed by the requirements to obtain controllably a square-pyramidal copper(II) centre containing a basal phenoxide ligand, and to prevent dimerisation through bridging of the co-ordinated phenoxide, which has hampered several previous model studies of GOase.[9,10,12,14–16] Both these criteria are met by complexes of stoichiometry [Cu(L)(Tp^{Ph})], where L is a bidentate ligand.[20,21] Salicylaldehydes and their Schiff bases were the bidentate phenols of choice, since methods for the synthesis and derivatisation of salicylaldehydes are well established. Hence, aminal protection of the 2-hydroxy-5-methylbenzaldehyde (HL^1)[22] carbonyl group allows directed lithiation and subsequent electrophilic substitution at the 3 position of the phenyl ring by MeEEMe (E = S or Se).[13] The protecting group is subsequently removed by acid hydrolysis to afford 2-hydroxy-5-methyl-3-methylsulfanylbenzaldehyde (HL^2) or 2-hydroxy-5-methyl-3-methylselanylbenzaldehyde (HL^3; Scheme 1). Schiff bases HL^4R and HL^5R (R = Me or Ph), derived from HL^1 and HL^2 respectively, were prepared in the usual way by treatment of the relevant aldehyde with RNH_2 in MeOH (Scheme 1). Since [Cu(L^5R)(Tp^{Ph})] complexes could not be prepared (see below), analogous Schiff bases derived from HL^3 were not pursued.

Complexation of $Cu(O_2CMe)_2\cdot H_2O$ by equimolar amounts of K[Tp^{Ph}][23] and HL^1, HL^4Me or HL^4Ph in CH_2Cl_2 at room temperature affords green solutions from which, after filtration and concentration of the filtrate, dark green crystalline solids can be obtained in 40–46% yields by addition of a large excess of hexanes and overnight storage at −30 °C. A small amount of mustard-coloured [Cu(Tp^{Ph})$_2$][24] precipitates immediately upon addition of hexanes, and can be removed by filtration of the solution before cold storage. This method was unsuccessful when employing HL^2 or HL^3 (see below); however, complexation of hydrated $Cu(BF_4)_2$ under the same conditions by 1 molar equivalent of K[Tp^{Ph}] and HL^2 or HL^3 did afford the desired deep yellow-green species, addition of 1 equivalent of Bu″$_4$NOH to the reaction giving improved yields and purity of product. We ascribe the moderate yields of these complexations to the high solubility of the dark green products **1**–**5** in all common organic solvents, which results in substantial solubility losses upon crystallisation.

The compounds were identified as the desired products [Cu(L)(Tp^{Ph})] ([L]$^-$ = [L^1]$^-$, **1**; [L^2]$^-$, **2**; [L^3]$^-$, **3**; [L^4Me]$^-$, **4** or [L^4Ph]$^-$, **5**) by the following criteria: IR spectroscopy, which demonstrated the presence of [Tp^{Ph}]$^-$ and the relevant bidentate ligand; FAB mass spectrometry which, although giving complex spectra, showed strong molecular ions corresponding to [^{63}Cu(L)(Tp^{Ph})]$^+$ ([L]$^-$ = [L^1]$^-$, *m*/*z* = 639; [L^2]$^-$, *m*/*z* = 685; [L^3]$^-$, *m*/*z* = 733; [L^4Me]$^-$, *m*/*z* = 652; [L^4Ph]$^-$, *m*/*z* = 714); and CHN microanalysis, which was consistent with the proposed formulations. As we have observed previously,[20] although the ν(B–H) vibrations in solid **1**–**5** varied widely, in CH_2Cl_2 solution virtually identical IR spectra in the range 2 600–2 200 cm^{-1} were obtained for all five compounds.

Attempts to prepare **2**, **3** or analogous complexes containing [L^5Me]$^-$ or [L^5Ph]$^-$ from $Cu(O_2CMe)_2\cdot H_2O$ cleanly afforded in all cases a blue-green crystalline product identified as [Cu(O_2CMe)(Hpz^{Ph})(Tp^{Ph})] (Hpz^{Ph} = 3-phenylpyrazole) by comparison with a genuine sample.[24] Presumably, this complex arises from copper-assisted B–N bond cleavage by the hindered Brønsted-acidic phenols, since complexation of $Cu(O_2CMe)_2\cdot H_2O$ by K[Tp^{Ph}] only under these conditions yields [Cu(O_2CMe)(Tp^{Ph})].[25] Brønsted or Lewis acid-catalysed degradation of tris(pyrazolyl)borates is a well known feature of their co-ordination chemistry.[25,26] In an attempt to avoid unwanted anion-containing species, $Cu(BF_4)_2\cdot xH_2O$ was complexed with 1 equivalent of K[Tp^{Ph}] and HL^5Me or HL^5Ph in CH_2Cl_2 in the presence or absence of added base. However, **2** was the only copper(II) product isolated from these reactions, reflecting hydrolysis of the [L^5R]$^-$ (R = Me or Ph) imine moieties during the reaction. Our inability to prepare [Cu(L^5R)(Tp^{Ph})] probably reflects unfavourable steric interactions between the Schiff base and [Tp^{Ph}]$^-$ ligands; this is discussed below.

Single crystal structures

Single crystal structure determinations were carried out on complexes **1**, **2**, **4** and **5**. Views of the molecular structures of **1**, **4** and **5** in the crystal are shown in Figs. 2–4, while selected metric parameters are given in Table 1. The structure of **2** has been presented previously.[19]

Compound **1** in the crystal is very similar to **2** (Fig. 2). The complex shows a fairly regular square pyramidal geometry, the copper(II) ion being co-ordinated by 3 pyrazole N-donors, and the phenoxide and carbonyl O atoms of the salicylaldehyde ligand. There is a lengthened apical Cu(1)–N(12) bond of

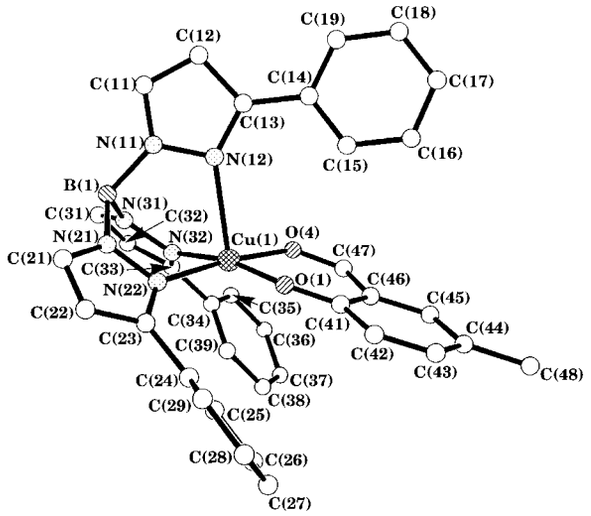

Fig. 2 Structure of the $[Cu(L^1)(Tp^{Ph})]$ complex molecule in the crystal of $\mathbf{1}\cdot CH_2Cl_2$, showing the atom numbering scheme employed. For clarity, all hydrogen atoms have been omitted.

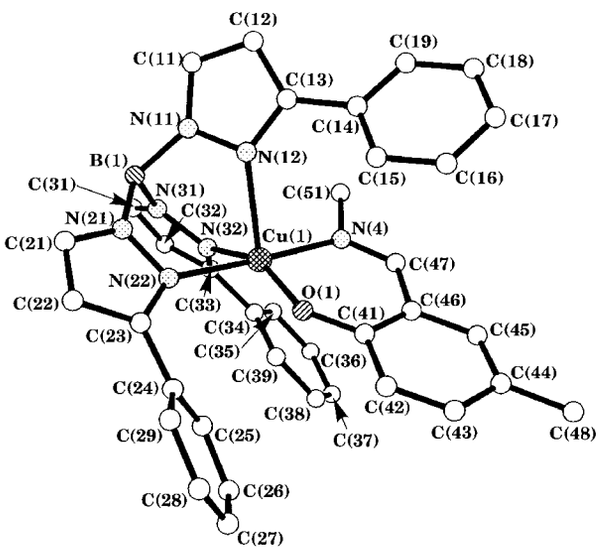

Fig. 3 Structure of the $[Cu(L^4Me)(Tp^{Ph})]$ complex molecule in the crystal of $\mathbf{4}\cdot CH_2Cl_2$. Details as for Fig. 2.

2.399(7) Å compared to that of **2** [2.337(6) Å]; this is reflected in the pitch of the apical $[Tp^{Ph}]^-$ phenyl substituent C(14)–C(19), which makes a dihedral angle of 19.8(6)° to the apical pyrazole ring [N(11), N(12), C(11)–C(13)] in **1**, compared to 31.0(4)° in **2**. The decreased steric interactions between the apical phenyl group and $[L^1]^-$ cause the plane of the bidentate ligand to be bent away from the basal plane of the molecule to a lesser extent in **1** compared to that of $[L^2]^-$ in **2**. Hence, the dihedral angle between the least squares planes formed by [O(1), O(4), C(41)–C(48)] and by [Cu(1), N(22), N(32), O(1), O(4)], is 19.7(3)° in **1** while for **2** it is 28.2(3)°. The other bond lengths to Cu(1) in **1** and **2** are crystallographically indistinguishable, while bond angles at Cu(1) show variations between the two structures of <3°. The difference between the basal *trans* angles N(22)–Cu(1)–O(4) and N(32)–Cu(1)–O(1) in **1** is 4.6°, the basal donors hence being only slightly twisted away from planarity. The apical pyrazole ring is effectively perpendicular to the basal planes of the complex, the dihedral angle formed between the planes [N(11), N(12), C(11)–C(13)] and [Cu(1), N(22), N(32), B(1)] being 88.3(3)°.

In contrast, the structure of complex **4** exhibits a much more distorted stereochemistry at copper (Fig. 3). The distribution of bond lengths is the same as for **1** and **2** (Table 1), suggesting that the co-ordination geometry of **4** is still derived from a square

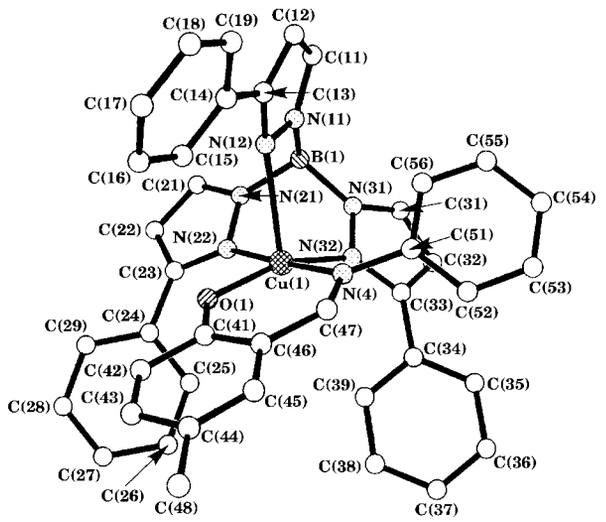

Fig. 4 Structure of the $[Cu(L^4Ph)(Tp^{Ph})]$ complex molecule in the crystal of **5**. Details as for Fig. 2.

pyramid. However, the basal plane of the complex is now substantially twisted, the difference between the *trans* angles N(22)–Cu(1)–N(4) and N(32)–Cu(1)–O(1) being 22.6°. The plane of the apical pyrazole ring [N(11), N(12), C(11)–C(13)] forms a dihedral angle of 79.2(1)° with the least squares plane [Cu(1), N(22), N(32), B(1)], reflecting steric repulsions between this ring and the $[L^4Me]^-$ methyl group. Interestingly, however, this distortion is accompanied by a 0.1 Å shortening of the apical Cu(1)–N(12) bond compared to **1**, to 2.299(2) Å.

The structure of complex **5** (Fig. 4) shows a less severe basal twist compared to that of **4**, in that the difference between the *trans* angles N(22)–Cu(1)–N(4) and N(32)–Cu(1)–O(1) is 17.9°. The apical Cu(1)–N(12) bond is 0.13 Å longer than for **4**, at 2.434(3) Å, while the apical pyrazole moiety [N(11), N(12), C(11)–C(13)] is now perpendicular to the basal plane of the $[Tp^{Ph}]^-$ group [dihedral angle 88.6(2)°]. This pyrazole ring is in close contact with H(56) of the $[L^4Ph]^-$ phenyl substituent (not shown in Fig. 4), which lies 2.47 Å from the [N(11), N(12), C(11)–C(13)] centroid; the dihedral angle of 100.8(2)° between C(51)–C(56) and [N(11), N(12), C(11)–C(13)] indicates a significant edge-to-face π–π interaction. There is also a graphitic interaction between C(51)–C(56) and the $[Tp^{Ph}]^-$ phenyl ring C(34)–C(39) which lie 3.2 Å apart, the dihedral angle between the planes of these two groups being 6.9(2)° and the centroids of the two rings being offset by 3.3 Å.[27]

The molecular distortions present in complexes **4** and **5** can be attributed to the steric effects of the $[L^4R]^-$ *N*-methyl or *N*-phenyl substituents, which lie wedged between basal [N(31), N(32), C(31)–C(33)] and apical [N(11), N(12), C(11)–C(13)] arms of the $[Tp^{Ph}]^-$ tripod. Since the Schiff base linkage is coplanar with the phenoxide ring, the effect of this is to orient the $[L^4R]^-$ ligand so that the phenoxide donor O(1) is forced 0.83 (R = Me) or 0.69 Å (R = Ph) below the basal plane formed by Cu(1), N(4), N(22) and N(32). The increased basal twist in **4** compared to that in **5** may also reflect the steric consequences of the shortened apical Cu-N bond in the former complex (*cf.* **1** and **2**, see above). Space-filling models show that the C(42)–H(42) bond points towards the C(24)–C(29) phenyl substituent in **4** and **5**, the distance between H(42) and the centroid of this phenyl ring being 3.1 (R = Me) and 3.5 Å (R = Ph). This explains our inability to prepare $[Cu(L^5R)(Tp^{Ph})]$ (R = Me or Ph), since the thioether substituent at the 3 position of the $[L^5R]^-$ phenoxide group would point directly into the C(24)–C(29) ring, rather than lying above it as in **2**.[19]

UV/visible and EPR spectroscopy

The d–d spectra of complexes **1**–**5** in CH_2Cl_2 at 293 K show a

Table 1 Bond lengths (Å) and angles (°) at copper in the single crystal structures

	[Cu(L^1)(Tp^{Ph})] **1** [a]	[Cu(L^2)(Tp^{Ph})] **2** [a,b]	[Cu(L^{4}Me)(Tp^{Ph})] **4** [c]	[Cu(L^{4}Ph)(Tp^{Ph})] **5** [c]
Cu(1)–N(12)	2.399(7)	2.337(6)	2.299(2)	2.434(3)
Cu(1)–N(22)	2.023(7)	2.009(6)	2.056(2)	2.054(3)
Cu(1)–N(32)	1.997(7)	1.996(7)	2.038(2)	1.992(3)
Cu(1)–O(1)	1.907(6)	1.941(7)	1.893(2)	1.885(3)
Cu(1)–X(4)	1.974(6)	1.967(5)	1.986(2)	2.013(3)
N(12)–Cu(1)–N(22)	89.6(3)	89.7(2)	86.82(8)	83.21(11)
N(12)–Cu(1)–N(32)	89.2(3)	90.0(2)	92.48(9)	96.80(12)
N(12)–Cu(1)–O(1)	101.7(2)	102.8(2)	111.57(9)	102.50(11)
N(12)–Cu(1)–X(4)	97.0(3)	98.7(2)	90.74(9)	95.04(11)
N(22)–Cu(1)–N(32)	88.5(3)	87.7(3)	85.01(9)	84.63(12)
N(22)–Cu(1)–O(1)	88.3(3)	91.5(3)	88.94(9)	89.80(12)
N(22)–Cu(1)–X(4)	173.2(3)	171.3(2)	177.41(8)	177.03(12)
N(32)–Cu(1)–O(1)	168.6(3)	167.1(2)	154.84(9)	159.14(12)
N(32)–Cu(1)–X(4)	90.1(3)	89.9(2)	94.25(9)	93.21(13)
O(1)–Cu(1)–X(4)	91.8(2)	88.9(3)	92.76(9)	92.92(12)

[a] X = O. [b] Ref. 19. [c] X = N

Table 2 X-Band EPR data for the complexes (10:1 CH_2Cl_2–toluene, 293 and 110 K). Hyperfine couplings are to ^{63,65}Cu and are in G

Complex	$\langle g \rangle$	$\langle A \rangle$	$g_\parallel$	$A_\parallel$	$g_\perp$
1 [Cu(L^1)(Tp^{Ph})]	2.142	60	2.284	160	2.065
2 [Cu(L^2)(Tp^{Ph})]	2.144	60	2.286	163	2.065
3 [Cu(L^3)(Tp^{Ph})]	2.144	61	2.289	164	2.065
4 [Cu(L^{4}Me)(Tp^{Ph})]	2.130	70	2.252	180	2.060
5 [Cu(L^{4}Ph)(Tp^{Ph})]	2.137	70	2.271	170	2.060

single absorption. This peak occurs at an identical wavelength and intensity for **1** and **2**, at $\lambda_{max} = 685 \pm 1$ nm ($\varepsilon_{max} = 92$–93 M^{-1} cm^{-1}), which is consistent with their essentially identical co-ordination spheres at copper in the crystal.[19] This strongly suggests that in solution the [L^2]$^-$ ligand in **2** is co-ordinated *via* both O-donors, as in the solid, rather than the phenoxide O and thioether S atom. The d–d bands shown by **3**–**5** lie at lower wavelength, occurring at $\lambda_{max} = 669$ nm ($\varepsilon_{max} = 110$ M^{-1} cm^{-1}) for **3**, 642 nm (148) for **4** and 664 nm (92) for **5**. For **4** and **5** these differences are probably related to the more distorted co-ordination geometries adopted by these complexes. The lower d–d wavelength for **3** compared to those of **1** and **2** may reflect similar structural distortions caused by steric repulsions between the large [L^3]$^-$ Se atom and a [Tp^{Ph}]$^-$ phenyl substituent. The UV/vis spectra of **1**–**5** also contain: an absorption at $\lambda_{max} = 390$–441 nm (3 400–5 100 M^{-1} cm^{-1}), which for **1** and **3** exhibits a high-wavelength shoulder and which arises from $\pi \longrightarrow \pi^*$ [28] and $\sigma(O) \longrightarrow d$ [11] transitions associated with the phenoxide ligands; one or (for **3**) two phenoxide $\pi \longrightarrow \pi^*$ transitions at $\lambda_{max} = 290$–329 nm (2 700–8 200 M^{-1} cm^{-1});[28] and a $\pi \longrightarrow \pi^*$ shoulder at $\lambda_{max} = 254$ nm from the [Tp^{Ph}]$^-$ phenyl substituents.[18,25]

EPR Data for complexes **1**–**5** in 10:1 CH_2Cl_2–toluene solution are listed in Table 2. In mobile solution 4-line spectra are observed as expected from coupling to ^{63,65}Cu ($I = 3/2$), while as frozen glasses the complexes exhibit axial spectra typical of tetragonal $\{d_{x^2-y^2}\}^1$ or $\{d_{xy}\}^1$ copper(II) centres;[29] **4** and **5** show slightly reduced $g_\parallel$ and increased A values compared to those of **1**–**3**. The axial symmetry of the g tensors was confirmed by running spectra of **1**, **2**, **4** and **5** at Q band, which gave g and $A_\parallel$ values indistinguishable from those of the X-band analyses. The isotropic and anisotropic spectra of **1**–**3** are essentially identical, again consistent with identical modes of co-ordination of [L^1]$^-$–[L^3]$^-$ in solution for these complexes. No superhyperfine coupling to ^{14}N ($I = 1$) was resolvable in any of these spectra, preventing more detailed EPR characterisation of **1**–**5** in solution. However, we have previously demonstrated that a closely related series of [Cu(L)(Tp^{Ph})] (L = bidentate ligand) complexes cleanly retain their square pyramidal structures upon dissolution.[20] Given the EPR and UV/vis data described here, which are entirely consistent with the co-ordination geometries in the crystal structures described above, it is very likely that the same is true for **1**–**5**.

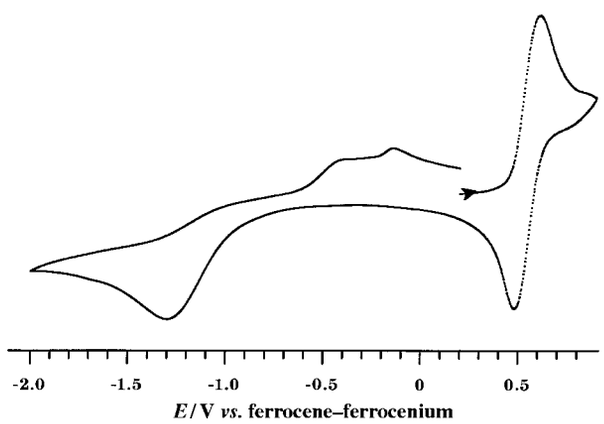

Fig. 5 Cyclic voltammogram of [Cu(L^2)(Tp^{Ph})] **2** in CH_2Cl_2–0.5 M $Bu^n_4NPF_6$ at 293 K, scan rate 100 mV s^{-1}.

Electrochemistry

Cyclic voltammograms of the phenol ligands and complexes in this study were run in CH_2Cl_2–0.5 M $NBu^n_4PF_6$ or MeCN–0.1 M $NBu^n_4PF_6$ at 293 K. The electrochemical data thus obtained are summarised in Table 3. Each of the bidentate ligands HL^1–HL^{5}R exhibits a 1-electron oxidation in CH_2Cl_2, corresponding to the proton-coupled oxidation of the neutral phenol to a phenoxyl radical. For HL^2 only this is a quasi-reversible process, showing $I_{p_c} : I_{p_a} = 0.2$ at 100 mV s^{-1} which increases only slightly at 1 V s^{-1}; an essentially identical $I_{p_c} : I_{p_a}$ ratio and half-potential is observed in MeCN for this couple. For the other ligands this oxidation is irreversible at scan rates up to 1 V s^{-1}. Comparison of the peak potentials for HL^1–HL^{5}R shows that *ortho*-methylsulfanyl or methylselanyl substitution of the phenoxide ring, and imination of the aldehyde function, each lower E_{p_a} by 250–550 mV; the former result is broadly in agreement with previous studies.[11,13,14,16] No secondary anodic processes were detected, although HL^3, HL^{4}R and HL^{5}R (R = Me or Ph) exhibit weak daughter reductions of unknown origin.

The cyclic voltammograms of complexes **1**–**5** in CH_2Cl_2 exhibit a 1-electron oxidation attributable to the conversion of the co-ordinated phenoxide ligand into a neutral radical. For **1** and **3**–**5** this is an irreversible process at scan rates up to 1 V s^{-1}. However, for **2** this oxidation is chemically reversible at 10 mV $s^{-1} \leq v \leq 1$ V s^{-1} (v = scan rate) and does not decrease in intensity upon repeated scanning (Fig. 5). In MeCN the **2**–[**2**]$^+$

Table 3 Voltammetric data for the compounds obtained in CH_2Cl_2–0.5 M $NBu^n_4PF_6$ or MeCN–0.1 M $NBu^n_4PF_6$ at 298 K. Potentials are quoted *vs.* an internal ferrocene–ferrocenium standard, at scan rate 100 mV s^{-1}

Compound	Solvent	$[L]^- \longrightarrow L^{\bullet} + e$ E_{p_a}/V (daughter E_{p_c}/V)	Secondary oxidation E_{p_a}/V	$Cu^{II/I}$ couple E_{p_c}/V (daughter E_{p_a}/V)
HL^1	CH_2Cl_2	+1.33	—	—
HL^2	CH_2Cl_2	+1.07[a]	—	—
	MeCN	+1.06[a]	—	—
HL^3	CH_2Cl_2	+1.04 (+0.60, −0.17)	—	—
HL^4Me	CH_2Cl_2	+1.06 (−1.53)	—	—
HL^4Ph	CH_2Cl_2	+1.08 (−0.79)	—	—
HL^5Me	CH_2Cl_2	+0.56 (−1.53)	—	—
HL^5Ph	CH_2Cl_2	+0.60 (−0.78)	—	—
1 $[Cu(L^1)(Tp^{Ph})]$	CH_2Cl_2	+0.84	+1.14	−1.39 (−0.34, −0.10)
2 $[Cu(L^2)(Tp^{Ph})]$	CH_2Cl_2	+0.53[b]	+1.26	−1.29 (−0.41, −0.11)
	MeCN	+0.55	—	−1.32 (−0.57, −0.17)
3 $[Cu(L^3)(Tp^{Ph})]$	CH_2Cl_2	+0.53 (−0.76)	+0.95	−1.31 (−0.35, −0.13)
4 $[Cu(L^4Me)(Tp^{Ph})]$	CH_2Cl_2	+0.59	+1.08	−1.57 (−0.74, −0.07)
5 $[Cu(L^4Ph)(Tp^{Ph})]$	CH_2Cl_2	+0.65	—[c]	−1.40 (−0.07)

[a] Quasi-reversible process, $E_{\frac{1}{2}}$ value quoted. [b] Chemically reversible process, $E_{\frac{1}{2}}$ value quoted. [c] Secondary oxidation present as a broad rise in the baseline, with no obvious peak maximum.

oxidation occurs at an identical anodic peak potential as in CH_2Cl_2, but is now irreversible. This probably reflects displacement of the phenoxyl ligand by the co-ordinating MeCN solvent, and its rapid subsequent decomposition, following electrooxidation.[20]

The peak potentials for the ligand oxidations of complexes **1**–**5** are 0.4–0.5 V less positive than for the corresponding "free" ligand, which is inconsistent with previous suggestions that metallation of a phenoxide should have an equivalent effect to protonation on its redox chemistry.[12,14] Possibly, back donation into the π* orbital of the co-ordinated C=O or C=N bond has a significant role in lowering E_{p_a} of co-ordinated $[L^1]^-$–$[L^4R]^-$. Complexes **1**–**5** in CH_2Cl_2 also exhibit a second irreversible oxidation of variable broadness and intensity, which is not shown by the "free" ligands; for **2**, scanning past this potential greatly reduces the intensity of the return peak for the first oxidation. The origin of this broad, irreversible wave is unclear, although similar processes have been previously observed in the voltammograms of other phenols and their complexes.[12,15,30] No such secondary process was observed for **2** in MeCN.

It is interesting to compare the cyclic voltammogram of complex **2** with that of the closely related compound [Cu(*O*,*S*-OC_6H_4SMe-2)($Tp^{Cum,Me}$)] {$[Tp^{Cum,Me}]^-$ = hydridotris[3-(4-isopropylphenyl)-5-methylpyrazol-1-yl]borate}, which exhibits an irreversible ligand oxidation at E_{p_a} = +0.61 V under the same conditions.[18] The decreased stability of the latter complex towards oxidation might originate from co-ordination of the phenoxide thioether substituent to the copper(II) ion, which forces the SMe group out of the plane of the phenoxide ring with a C(*ortho*)–C(*ipso*)–S–C(methyl) torsion of 72°. This would reduce conjugation of the sulfur atom with the phenoxide ring, thus limiting its ability to stabilise the π-symmetry unpaired spin on the phenoxyl oxidation product.

In addition to the ligand oxidations, complexes **1**–**5** show an irreversible 1-electron process between E_{p_c} = −1.3 and −1.6 V, assignable to a $Cu^{II/I}$ reduction, with an associated daughter peak at E_{p_a} = −0.1 V (Fig. 5); for **1**–**4**, an additional weaker daughter at a more negative potential was also observed (Table 3). Repeated scanning over the range $-1.7 \leq E \leq +0.2$ V caused no decay in intensity of these peaks, demonstrating the overall chemical reversibility of this process. The observation of a common $Cu^{I/II}$ daughter peak for **1**–**5** suggests that reduction to Cu^I may be accompanied by dissociation of the phenoxide ligand, giving [Cu(solv)(Tp^{Ph})] (solv = solvent)[31,32] or [{Cu(Tp^{Ph})}$_2$][32,33] as the major product. However, the −0.1 V reoxidation potential of this daughter is more negative than oxidation potentials reported for other copper(I) pyrazolylborate complexes, which show $+0.2 \leq E_{p_a}\{Cu^{I/II}\} \leq +0.5$ V in CH_2Cl_2.[32] Hence, the nature of the copper(I) daughter product at E_{p_a} = −0.1 V remains uncertain.

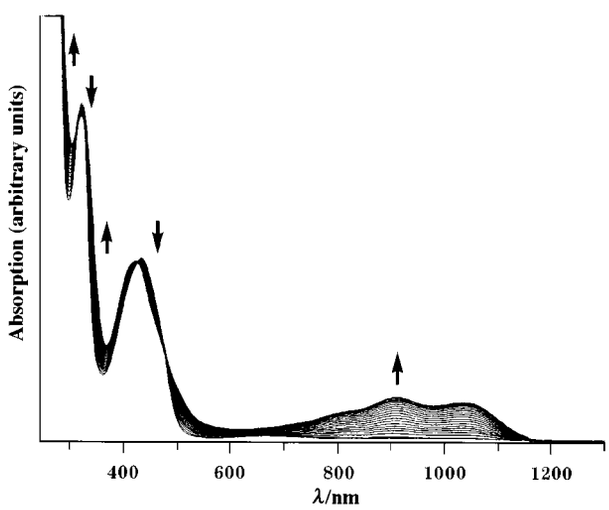

Fig. 6 Oxidation of complex **2** to $[2]^+$ by controlled potential electrolysis in CH_2Cl_2–0.5 M $NBu^n_4PF_6$ at 243 K.

Controlled potential electrolysis of a CH_2Cl_2–0.5 M $NBu^n_4PF_6$ solution of complex **2** at 243 K at a potential corresponding to the reversible oxidation yields a brown solution which shows only a residual EPR signal from unchanged **2**. A similar experiment at the same temperature using an optically transparent electrode results in a shift of the $[L^2]^-$-derived absorptions to lower wavelength, with the concomitant appearance of new intense higher wavelength peaks (Fig. 6). The oxidised solution shows λ_{max} = 317 nm ($\varepsilon_{max} \approx 9\ 000\ M^{-1}\ cm^{-1}$), 419 (4 400), 470 (sh), 725 (sh), 818 (sh), 907 (1 200) and 1 037 (1 100) at 243 K. This transformation is not quite isosbestic (Fig. 6), reflecting slow decomposition of the product, which has an estimated half-life of *ca.* 10 h under these conditions. However, rereduction of this solution at 0 V immediately following oxidation regenerates **2** in >90% yields, demonstrating the good chemical reversibility of the **2**–$[2]^+$ couple. These observations are consistent with the formulation of $[2]^+$ as the antiferromagnetically coupled species $[Cu^{II}(L^{2\bullet})(Tp^{Ph})]^+$.[11,15,17] Attempts chemically to generate or isolate $[2]^+$ have thus far been unsuccessful.

Calculations

The 1-electron oxidations of HL^3 and [Cu(L^3)(Tp^{Ph})] occur at essentially identical potentials to those of their thioether-substituted analogues (Table 3). However, from the irreversible

nature of these processes for the former compounds it is clear that free or co-ordinated $L^{3\bullet}$ is much less kinetically stable than $L^{2\bullet}$ under our conditions. In order to rationalise these differences, and to predict the metal-binding properties of the radical ligands, EHMO calculations were performed on the "free" ligands HL (HL^1, HL^2 or HL^3) and the corresponding anions L^- and radicals $L^\bullet$. The calculated HOMO energies of HL^1 (−13.3), HL^2 (−11.9) and HL^3 (−12.1 eV) broadly support the observed trend for the oxidation potentials of these ligands, namely $HL^1 > HL^2 \approx HL^3$ (Table 3). The net atomic charges at O7 and O12 in HL (−0.8 and −1.1, respectively), L^- (−1.4 and −1.1) and $L^\bullet$ (−1.2 and −1.1) are identical for all three ligands. The small changes observed in these charges upon formation of $L^\bullet$, coupled with the lack of any other concentration of negative charge in the $L^\bullet$ molecules, strongly suggest that $L^\bullet$ in $[\mathbf{2}]^+$ should retain the *O*,*O*′-bidentate mode of co-ordination adopted in **2** (see above).

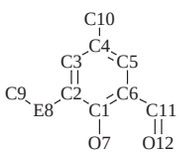

For all three $L^\bullet$ species the SOMO is of π symmetry, and is localised almost exclusively on the benzene ring and (for $L^{2\bullet}$ and $L^{3\bullet}$) chalcogen atom (Fig. 7). It is clear from a Mulliken analysis of the SOMO (Fig. 7) that the thioether substituent on $L^{2\bullet}$ accepts a substantially greater proportion of the phenoxyl unpaired spin than the selenoether group in $L^{3\bullet}$. Thus, the calculated fractional unpaired spin population (ρ) at S8 in $L^{2\bullet}$ is much greater than for Se8 in $L^{3\bullet}$ (Fig. 7). This trend is mirrored in the net atomic charge at E(8) in $L^\bullet$ (E = S, L = L^2; E = Se, L = L^3), which is substantially more positive for E = S than for E = Se. By comparison, higher level calculations on thioether-substituted phenoxyls by others have predicted $\rho(S) = 0.17$–0.28,[16,34] a suggestion confirmed by ENDOR spectroscopy.[35]

The unpaired spin population ρ(C4) of the benzaldehyde ring, *i.e. para* to the phenoxyl O atom (the most reactive site of a phenoxyl radical[36]), is greater in $L^{3\bullet}$ than in $L^{2\bullet}$ (Fig. 7). It is therefore clear that $L^{3\bullet}$ should be more reactive than $L^{2\bullet}$ towards dimerisation or recombination reactions. It is also noteworthy that ρ(C2) is greater for $L^{3\bullet}$ than for $L^{1\bullet}$ or $L^{2\bullet}$ (Fig. 7), which suggests that $L^{3\bullet}$ may also be more susceptible to degradation by C2–E8 (E = S or Se) bond homolysis than $L^{2\bullet}$. Both these observations predict an increased reactivity for $L^{3\bullet}$ compared to $L^{2\bullet}$, in agreement with observation. Therefore, from these electrochemical and theoretical results, we predict that a Cys-228Secys GOase mutant should form an oxidised Cu^{II}/[Tyr-272]$^\bullet$ species under identical conditions to the native enzyme, but that the resultant tyrosyl radical may be shorter lived.

Concluding remarks

Owing to our inability to crystallise $[\mathbf{2}]^+$, the lack of a spectroscopic handle for the copper(II) ion means that the precise molecular structure of this radical complex is uncertain. However, we can make the following observations. First, given the good chemical reversibility of the preparative **2**–$[\mathbf{2}]^+$ couple, solvolysis or intermolecular ligand exchange reactions following oxidation do not take place. Secondly, co-ordination of the poorly nucleophilic solvent employed (CH_2Cl_2) to the copper(II) ion following oxidation to yield a six-co-ordinate metal centre is very unlikely. Thirdly, of the >20 $[Cu(L)(Tp^R)]^{n+}$, $[CuX(L')(Tp^R)]$ or $[\{Cu(\mu\text{-}X)(Tp^R)\}_2]$ (R = alkyl or aryl, L = bidentate ligand, L′ = monodentate ligand, X = anion, $n = 0$ or 1) complexes structured in this work, and previously by us[20,24,25] and others,[18,21,37] all have essentially square pyramidal geometries at copper. This suggests that the copper(II) centre in $[\mathbf{2}]^+$ will retain the square-pyramidal stereochemistry adopted by **2**. Fourthly, since the calculated atomic charges at O7 and O12 in HL^2 and $L^{2\bullet}$ are essentially the same (see above), the $L^{2\bullet}$ ligand in $[\mathbf{2}]^+$ probably retains the *O*,*O*′-co-ordination mode found in **2**, rather than undergoing linkage isomerism to an *O*,*S*- or monodentate *O*-bound form. All of these facts are consistent with the molecular connectivities of **2** and $[\mathbf{2}]^+$ being identical.

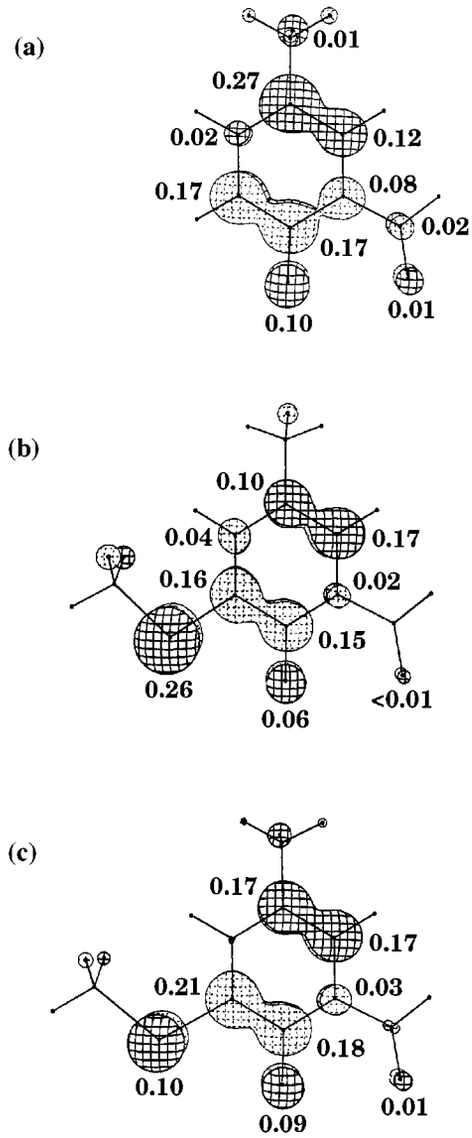

Fig. 7 EHMO Singly occupied molecular orbitals (SOMOs) for $L^{1\bullet}$, $L^{2\bullet}$ and $L^{3\bullet}$, showing the Mulliken unpaired spin populations. Contributions to the SOMO from H atoms, which are all ≤0.01, are not listed.

The UV/vis spectrum of $[\mathbf{2}]^+$ has the same form as those of other copper(II) phenoxyl GOase model compounds, which exhibit phenoxyl-derived absorptions near $\lambda_{max} = 400$ and 650 nm[11,15,17] that closely resemble those of unco-ordinated phenoxyls bearing alkyl substituents.[36] Although the spectrum of $[\mathbf{2}]^+$ differs from these literature compounds in that the higher wavelength absorption is broadened and being red-shifted by *ca.* 250 nm, the position of this peak almost exactly matches that observed for metal-free *ortho*-thioether-substituted phenoxyls,[12,16] as well as that of the Tyr-272 radical in holo- and apo-GOase.[6] Therefore, the high wavelength of the vis/NIR absorption of $[\mathbf{2}]^+$ is almost certainly a reflection of thioether substitution at the phenoxyl ligand. By analogy with the spectra of holo- and apo-GOase,[6] the structured appearance of this band probably results from co-ordination of the $L^{2\bullet}$ radical, and may reflect the superposition of MLCT and/or LMCT transitions involving $L^{2\bullet}$ onto the $\pi \longrightarrow \pi^*$ envelope.

The assignment of the vis/NIR absorptions exhibited by active GOase has been uncertain. In addition to the aforementioned $\pi \longrightarrow \pi^*$ and charge-transfer transitions involving Tyr-272 radical and the copper ion, a recent resonance Raman study suggested that this absorption is dominated by a Tyr-495→Tyr-272 radical (Fig. 1) LLCT process.[38] This idea appears to be supported by the fact that binding of azide to active GOase, which is accompanied by displacement of Tyr-495 from the Cu, causes a threefold reduction in intensity of the vis/NIR band to $\varepsilon_{max} \approx 1\ 000\ M^{-1}\ cm^{-1}$.[1,39] This reduced intensity is of similar magnitude to that shown by $[2]^+$, which does not have a phenoxide or similar π donor as apical ligand and so cannot undergo such an LLCT process. We are currently preparing new model compounds designed to reproduce the complete copper(II)/phenoxyl/tryptophan radical architecture in GOase, which will further address this question.

Experimental

Unless stated otherwise, all manipulations were performed in air using commercial grade solvents. 2-Hydroxy-5-methylbenzaldehyde (HL^1),[22] $K[Tp^{Ph}]$[23] and $[Cu(O_2CMe)(Tp^{Ph})]$[25] were prepared by the literature procedures; $Cu(O_2CMe)_2\cdot H_2O$ (Avocado), *N*,*N*′-dimethyl-1,2-diaminoethane (DMEDA), dimethyl disulfide, dimethyl diselenide, methylamine (1.0 M solution in MeOH), phenylamine, Bu^n_4NOH (1.0 M solution in MeOH) and $Cu(BF_4)_2\cdot xH_2O$ ($x \approx 4$; Aldrich) were used as supplied.

Syntheses

2-(2-Hydroxy-5-methylphenyl)-1,3-dimethylimidazolidine. The compound HL^1 (10.0 g, 7.35×10^{-2} mol) and DMEDA (7.5 g, 7.35×10^{-2} mol) were stirred in a suspension of $MgSO_4$ in absolute EtOH (250 cm^3) at room temperature for 16 h. The solution was filtered, and the filtrate evaporated to dryness to give a yellow oil that formed a waxy solid during storage at −30 °C and was analysed without further purification. Yield 14.9 g, 100% (Found: C, 69.7; H, 8.9; N, 13.8. Calc. for $C_{12}H_{16}N_2O$: C, 69.9; H, 8.8; N, 13.6%), mp *ca.* 15 °C. FAB mass spectrum: *m*/*z* 207, $[M + H]^+$; 206, $[M]^+$ and 205, $[M - H]^+$. NMR spectra $[(CD_3)_2SO$, 293 K]: ^1H, δ 11.0 (v br, 1 H, OH), 6.60 (dd, 8.2 and 2.1 Hz, 1 H, H^4), 6.83 (d, *J* 2.1, 1 H, H^6), 6.60 (d, *J* 8.2 Hz, 1 H, H^3), 3.40 (s, 1 H, CHN_2), 2.48–3.29 (m, 4 H, NCH_2), 2.20 (s, 3H, CH_3) and 2.15 (s, 6 H, NCH_3); ^{13}C, δ 155.8 (C^2), 131.0 (C^6), 129.8 (C^4), 126.3 (C^5), 120.6 (C^1), 115.7 (C^3), 90.6 (CHN_2), 51.8 (NCH_2), 38.6 (NCH_3) and 20.1 (CH_3).

2-Hydroxy-5-methyl-3-methylsulfanylbenzaldehyde (HL^2). To a mixture of 2-(2-hydroxy-5-methylphenyl)-1,3-dimethylimidazolidine (2.5 g, 1.21×10^{-2} mol) and TMEDA (5.6 g, 4.85×10^{-2} mol) in distilled Et_2O (150 cm^3) at −78 °C under N_2 was added Bu^nLi (32.3 cm^3 of a 1.5 M solution in hexanes, 4.85×10^{-2} mol). The solution was allowed to warm to room temperature and stirred for 6 h, during which time the initial precipitate dissolved and the solution slowly became orange. Dimethyl disulfide (5.7 g, 6.07×10^{-2} mol) was then carefully added (mildly exothermic), giving a yellow solution and white precipitate which was stirred overnight. The mixture was poured onto 2 M HCl (200 cm^3) and stirred for 10 min. The ether layer was separated, and the aqueous layer extracted 3 times with CH_2Cl_2. The combined organic extracts were dried over $MgSO_4$ and evaporated to dryness. The residue was dissolved in 2 : 1 hexanes–ethyl acetate and filtered through a silica plug. Evaporation of the solvent yielded a pungent oily yellow solid, which formed a yellow crystalline material upon washing with the minimum volume of hexanes. Yield 1.6 g, 73% (Found: C, 59.2; H, 5.5. Calc. for $C_9H_{10}O_2S$: C, 59.3; H, 5.5%), mp 80–81 °C. FAB mass spectrum: *m*/*z* 183, $[M + H]^+$; 182, $[M]^+$; 181, $[M - H]^+$; and 167, $[M - CH_3]^+$. NMR spectra $[(CD_3)_2SO$, 293 K]: ^1H, δ 10.99 (br, 1 H, OH), 9.99 (s, CH=O), 7.33 (s, 1 H), 7.31 (s, 1 H, $H^4 + H^6$), 2.42 (s, 3 H, SCH_3) and 2.29 (s, 3 H, CH_3); ^{13}C, δ 196.3 (CH=O), 155.0 (C^2), 133.5 (C^6), 129.5 (C^5), 128.7 (C^4), 127.0 (C^3), 120.3 (C^1), 20.0 (CH_3) and 13.9 (SCH_3). IR spectrum (Nujol): 1658s cm^{-1} (C=O).

2-Hydroxy-5-methyl-3-methylselanylbenzaldehyde (HL^3). Method as for HL^2, using dimethyl diselenide (11.4 g, 6.07×10^{-2} mol). The product was a yellow crystalline solid. Yield 1.4 g, 50% (Found: C, 46.9; H, 4.4. Calc. for $C_9H_{10}O_2Se$: C, 47.2; H, 4.4%), mp 85–86 °C. FAB mass spectrum: *m*/*z* 231, $[M + H]^+$; 230, $[M]^+$; and 215, $[M - CH_3]^+$. NMR spectra $[(CD_3)_2SO$, 293 K]: ^1H, δ 11.05 (br, 1 H, OH), 9.98 (s, CH=O), 7.38 (s, 1 H), 7.37 (s, 1 H, $H^4 + H^6$), 2.30 (s, 3 H) and 2.29 (s, 3 H, $CH_3 + SeCH_3$); ^{13}C, δ 196.4 (CH=O), 155.5 (C^2), 135.7 (C^6), 130.0 (C^5), 129.6 (C^4), 121.5 (C^3), 120.3 (C^1), 19.9 (CH_3) and 4.5 ($SeCH_3$). IR spectrum (Nujol): 1640s cm^{-1} (C=O).

(2-Hydroxy-5-methylbenzylidene)methylamine (HL^4Me). A MeOH (50 cm^3) solution of HL^1 (0.50 g, 3.68×10^{-3} mol) and $MeNH_2$ (4.0 cm^3 of a 1.0 M solution in MeOH, 4.0×10^{-3} mol) was left to stand at room temperature for 15 min. Evaporation of the solution to dryness afforded a yellow oil which was analysed without further purification. Yield 0.52 g, 95% (Found: C, 72.5; H, 7.4; N, 9.3. Calc. for $C_9H_{11}NO$: C, 72.5; H, 7.4; N, 9.4%). FAB mass spectrum: *m*/*z* 150, $[M + H]^+$; and 149, $[M]^+$. NMR spectra $[(CD_3)_2SO$, 293 K]: ^1H, δ 13.16 (s, 1 H, OH), 8.47 (s, 1 H, CH=N), 7.19 (d, 1.9 Hz, 1 H, H^6), 7.12 (dd, *J* 8.4 and 1.9, 1 H, H^4), 6.77 (d, *J* 8.4 Hz, 1 H, H^3), 3.42 (s, 3 H, NCH_3) and 2.23 (s, 3 H, CH_3); ^{13}C, δ 167.0 (CH=N), 158.3 (C^2), 132.8 (C^6), 131.3 (C^4), 126.9 (C^5), 118.4 (C^1), 116.2 (C^3), 45.5 (NCH_3) and 19.9 (CH_3).

(2-Hydroxy-5-methylbenzylidene)phenylamine (HL^4Ph). A MeOH (50 cm^3) solution of HL^1 (0.50 g, 3.68×10^{-3} mol) and $PhNH_2$ (0.34 g, 3.68×10^{-3} mol) was refluxed for 15 min. Evaporation of the solution to dryness afforded an orange oil which solidified upon trituration with Et_2O. Yield 0.61 g, 78% (Found: C, 79.6; H, 6.2; N, 6.7. Calc. for $C_{14}H_{13}NO$: C, 79.6; H, 6.2; N, 6.6%), mp 71–73 °C. FAB mass spectrum: *m*/*z* 212, $[M + H]^+$; 211, $[M]^+$; 210, $[M - H]^+$; 195, $[M - CH_3 - H]^+$; 134, $[M - C_6H_5]^+$; and 104, $[C_6H_5N{=}CH]^+$. NMR spectra $[(CD_3)_2SO$, 293 K]: ^1H, δ 12.78 (br, 1 H, OH), 8.88 (s, 1 H, CH=N), 7.42 (m, 5 H, H^6 + NPh $H^{2/6}$ + $H^{3/5}$), 7.31 (m, 1 H, NPh H^4), 7.22 (dd, *J* 8.4 and 1.8, 1 H, H^4), 6.87 (d, *J* 8.4 Hz, 1 H, H^3) and 2.26 (s, 3 H, CH_3); ^{13}C, δ 164.1 (CH=N), 158.9 (C^2), 149.1 (NPh C^1), 134.8 (C^6), 133.1 (C^4), 130.2 (NPh $C^{3/5}$), 128.4 (C^5), 127.6 (NPh C^4), 122.1 (NPh $C^{2/6}$), 119.8 (C^1), 117.2 (C^3) and 20.7 (CH_3).

(2-Hydroxy-5-methyl-3-methylsulfanylbenzylidene)methylamine (HL^5Me). Method as for HL^4Me, using HL^2 (0.67 g, 3.68×10^{-3}). The orange oil thus obtained was triturated with Et_2O to afford an orange solid. Yield 0.52 g, 73% (Found: C, 61.3; H, 6.6; N, 7.1. Calc. for $C_{10}H_{13}NOS$: C, 61.5; H, 6.7; N, 7.2%), mp 94–95 °C. FAB mass spectrum: *m*/*z* 196, $[M + H]^+$; 195, $[M]^+$; 194, $[M - H]^+$; 181, $[M - CH_3]^+$; and 162 $[M - SH]$. NMR spectra $[(CD_3)_2SO$, 293 K]: ^1H, δ 14.07 (br, 1 H, OH), 8.43 (s, 1 H, CH=N), 7.00 (s, 1 H), 6.95 (s, 1 H, Ph $H^4 + H^6$), 3.49 (s, 3 H, NCH_3), 2.36 (s, 3 H, SCH_3) and 2.23 (s, 3 H, CH_3); ^{13}C, δ 167.1 (CH=N), 158.4 (C^2), 129.1 (C^6), 127.6 (C^4), 126.5, 126.2 ($C^3 + C^5$), 116.1 (C^1), 43.6 (NCH_3), 20.2 (CH_3) and 13.6 (SCH_3).

(2-Hydroxy-5-methyl-3-methylsulfanylbenzylidene)phenylamine (HL^5Ph). Method as for HL^4Ph, using HL^2 (0.67 g, 3.68×10^{-3}). The product formed blood-red plates from Et_2O. Yield 0.67 g, 71% (Found: C, 69.9; H, 5.9; N, 5.4. Calc. for $C_{15}H_{15}NOS$: C, 70.0; H, 5.9; N, 5.4%), mp 74–75 °C. FAB mass spectrum: *m*/*z* 257, $[M + H]^+$; 256, $[M]^+$; 242, $[M - CH_3]^+$;

224, $[M - S]^+$; 211, $[M - SCH_3 + H]^+$; 180, $[M - C_6H_5]^+$; and 104, $C_6H_5N{=}CH$. NMR spectra $[(CD_3)_2SO$, 293 K]: ^1H, δ 13.90 (br, 1 H, OH), 8.90 (s, 1 H, CH=N), 7.45 (m, 4 H, NPh $H^{2/6}$ + $H^{3/5}$), 7.33 (m, 1 H, NPh H^4), 7.22 (d, 1.8 Hz, 1 H), 7.14 (d, *J* 1.8 Hz, 1 H, $H^4 + H^6$), 3.36 (s, 3 H, NCH_3), 2.43 (s, 3 H, SCH_3) and 2.29 (s, 3 H, CH_3); ^{13}C, δ 163.6 (CH=N), 155.5 (C^2), 147.3 (NPh C^1), 129.9 (C^6), 129.5 (NPh $C^{3/5}$), 128.8 (C^4), 128.0 (C^5), 127.2 (NPh C^4), 125.8 (C^3), 121.4 (NPh $C^{2/6}$), 117.5 (C^1), 43.6 (NCH_3), 20.2 (CH_3) and 13.7 (SCH_3).

[Hydridotris(3-phenylpyrazol-1-yl)borato](2-hydroxy-5-methylbenzaldehydato)copper(II) 1. A mixture of K[Tp^{Ph}] (0.50 g, 1.04×10^{-3} mol), HL^1 (0.14 g, 1.04×10^{-3} mol) and $Cu(O_2CMe)_2{\cdot}H_2O$ (0.21 g, 1.04×10^{-3} mol) was stirred in CH_2Cl_2 (20 cm^3) at room temperature for 1 h. The resultant dark green solution was filtered, reduced to *ca.* 5 cm^3 volume, and hexanes (100 cm^3) were added. A small amount of mustard-yellow powder precipitated immediately and was removed by filtration. Overnight storage of the filtrate at −30 °C yielded green microcrystals, which were recrystallised once from CH_2Cl_2–hexanes to remove a white sticky impurity. Yield 0.27 g, 41% (Found: C, 59.7; H, 4.3; N, 11.5. Calc. for $C_{35}H_{29}BCuN_6O_2{\cdot}CH_2Cl_2$: C, 59.7; H, 4.3; N, 11.6%). FAB mass spectrum: *m*/*z* 648, $[^{63}Cu(Hpz^{Ph})(H^{11}B\{pz^{Ph}\}_3)]^+$; 639, $[^{63}Cu(L^1)(H^{11}B\{pz^{Ph}\}_3)]^+$; 567, $[^{63}Cu_2(H^{11}B\{pz^{Ph}\}_3)]^+$; 504, $[^{63}Cu(H^{11}B\{pz^{Ph}\}_3)]^+$; 495, $[^{63}Cu(L^1)(H^{11}B\{pz^{Ph}\}_2)]^+$; and 361, $[^{63}Cu(H^{11}B\{pz^{Ph}\}_2)]^+$. UV/vis spectrum ($CH_2Cl_2$): λ_{max} = 254 nm (sh), 313 (sh), 409 (ε_{max} = 3 400 M^{-1} cm^{-1}), 427 (sh) and 684 (93). IR spectrum: (Nujol) 2 473w (B–H); (CH_2Cl_2) 2 490, 2 474 and 2 455 cm^{-1}.

[Hydridotris(3-phenylpyrazol-1-yl)borato](2-hydroxy-5-methyl-3-methylsulfanylbenzaldehydato)copper(II) 2. To a mixture of K[Tp^{Ph}] (0.50 g, 1.04×10^{-3} mol), HL^2 (0.19 g, 1.04×10^{-3} mol) and $Cu(BF_4)_2{\cdot}xH_2O$ (0.32 g, 1.04×10^{-3} mol) in CH_2Cl_2 (20 cm^3) was added Bu^n_4NOH (1.04 cm^3 of a 1.0 M solution in MeOH). The yellow suspension was stirred at room temperature for 30 min. The resultant dark yellow-green solution was filtered, concentrated to 5 cm^3 and worked up as described for complex **1**. The product formed dark green microcrystals from CH_2Cl_2–hexanes. Yield 0.30 g, 42% (Found: C, 63.0; H, 4.6; N, 13.4. Calc. for $C_{36}H_{31}BCuN_6O_2S$: C, 63.0; H, 4.6; N, 12.3%). FAB mass spectrum: *m*/*z* 710, $[^{63}Cu_2(Hpz^{Ph})(H^{11}B\{pz^{Ph}\}_3) - H]^+$; 685, $[^{63}Cu(L^2)(H^{11}B\{pz^{Ph}\}_3)]^+$; 648, $[^{63}Cu(Hpz^{Ph})(H^{11}B\{pz^{Ph}\}_3)]^+$; 541, $[^{63}Cu(L^2)(H^{11}B\{pz^{Ph}\}_2)]^+$; 567, $[^{63}Cu_2(H^{11}B\{pz^{Ph}\}_3)]^+$; 504, $[^{63}Cu(H^{11}B\{pz^{Ph}\}_3)]^+$; and 361, $[^{63}Cu(H^{11}B\{pz^{Ph}\}_2)]^+$. UV/vis spectrum ($CH_2Cl_2$): λ_{max} = 254 nm (sh), 319 (ε_{max} = 8 200 M^{-1} cm^{-1}), 437 (4 000) and 685 (92). IR spectrum: (Nujol) 2 451w (B–H); (CH_2Cl_2) 2 490, 2 473 and 2 455 cm^{-1}.

[Hydridotris(3-phenylpyrazol-1-yl)borato](2-hydroxy-5-methyl-3-methylselanylbenzaldehydato)copper(II) 3. Method as for complex **2**, employing HL^3 (0.23 g, 1.04×10^{-3} mol). The product formed dark green microcrystals from CH_2Cl_2–hexanes. Yield 0.32 g, 41% (Found: C, 57.6; H, 4.2; N, 11.2. Calc. for $C_{36}H_{31}BCuN_6O_2Se{\cdot}H_2O$: C, 57.6; H, 4.4; N, 11.1%). FAB mass spectrum: *m*/*z* 796, $[^{63}Cu_2(L^3)(H^{11}B\{pz^{Ph}\}_3)]^+$; 733, $[^{63}Cu(L^3)(H^{11}B\{pz^{Ph}\}_3)]^+$; 649, $[^{63}Cu(Hpz^{Ph})(H^{11}B\{pz^{Ph}\}_3) + H]^+$; 589, $[^{63}Cu(L^2)(H^{11}B\{pz^{Ph}\}_2) - H]^+$; 504, $[^{63}Cu(H^{11}B\{pz^{Ph}\}_3)]^+$; and 361, $[^{63}Cu(H^{11}B\{pz^{Ph}\}_2)]^+$. UV/vis spectrum ($CH_2Cl_2$): λ_{max} = 254 nm (sh), 290 (sh), 329 (ε_{max} = 5 400 M^{-1} cm^{-1}), 441 (3 900), 460 (sh) and 669 (110). IR spectrum: (Nujol) 2 465w (B–H); (CH_2Cl_2) 2 488, 2 472 and 2 455 cm^{-1}.

[Hydridotris(3-phenylpyrazol-1-yl)borato][(2-hydroxy-5-methylbenzylidene)methylamido]copper(II) 4. Method as for complex **1**, using HL^4Me (0.15 g, 1.04×10^{-3} mol). The product formed dark green crystals from CH_2Cl_2–hexanes. Yield 0.31 g, 46% (Found: C, 60.2; H, 4.6; N, 13.2. Calc. for $C_{36}H_{32}BCuN_7O{\cdot}CH_2Cl_2$: C, 60.2; H, 4.6; N, 13.3%). FAB mass spectrum: *m*/*z* 652, $[^{63}Cu(L^4Me)(H^{11}B\{pz^{Ph}\}_3)]^+$; 509, $[^{63}Cu(L^4Me)(H^{11}B\{pz^{Ph}\}_2)]^+$; and 361, $[^{63}Cu(H^{11}B\{pz^{Ph}\}_2)]^+$. UV/vis spectrum ($CH_2Cl_2$): λ_{max} = 254 nm (sh), 309 (ε_{max} = 2 700 M^{-1} cm^{-1}), 390 (5 100) and 642 (148). IR spectrum: (Nujol) 2 439w (B–H); (CH_2Cl_2) 2 486, 2 470 and 2 453 cm^{-1}.

[Hydridotris(3-phenylpyrazol-1-yl)borato][(2-hydroxy-5-methylbenzylidene)phenylamido]copper(II) 5. Method as for complex **1**, using HL^4Ph (0.22 g, 1.04×10^{-3} mol). The product formed dark green crystals from CH_2Cl_2–hexanes. Yield 0.32 g, 43% (Found: C, 67.3; H, 4.8; N, 13.5. Calc. for $C_{41}H_{34}BCuN_7O{\cdot}H_2O$: C, 67.2; H, 5.0; N, 13.4%). FAB mass spectrum: *m*/*z* 714, $[^{63}Cu(L^4Ph)(H^{11}B\{pz^{Ph}\}_3)]^+$; 648, $[^{63}Cu(Hpz^{Ph})(H^{11}B\{pz^{Ph}\}_3)]^+$; 570, $[^{63}Cu(L^4Ph)(H^{11}B\{pz^{Ph}\}_2)]^+$; 504, $[^{63}Cu(H^{11}B\{pz^{Ph}\}_3)]^+$; and 361, $[^{63}Cu(H^{11}B\{pz^{Ph}\}_2)]^+$. UV/vis spectrum ($CH_2Cl_2$): λ_{max} = 254 nm (sh), 295 (sh), 415 (ε_{max} = 3 400 M^{-1} cm^{-1}) and 664 (92). IR spectrum: (Nujol) 2 436w (B–H); (CH_2Cl_2) 2 486, 2 471 and 2 455 cm^{-1}.

Single crystal structure determinations

Single crystals of X-ray quality of complexes **1**·CH_2Cl_2 and **4**·CH_2Cl_2 were grown by diffusion of hexanes into CH_2Cl_2 solutions. Crystals of **5** were grown by layering a toluene solution with hexanes. Experimental details from the structure determinations are given in Table 4. All structures were solved by direct methods (SHELXTL Plus[40]) and refined by full matrix least squares on F^2 (SHELXL 93[41]), with H atoms placed in calculated positions.

During refinement of complex **1**, the CH_2Cl_2 solvent molecule was found to be disordered over two sites, which were modelled with a 60 : 40 occupancy ratio using common C–Cl and Cl ··· Cl distances of 1.70(2) and 2.78(2) Å respectively. All wholly occupied non-H atoms, together with the major orientation of the disordered solvent molecule, were modelled anisotropically. No disorder was detected in the structures **4** and **5** during refinement. All non-H atoms were refined anisotropically, and no restraints were applied.

CCDC reference number 186/1417.

See http://www.rsc.org/suppdata/dt/1999/1753/ for crystallographic files in .cif format.

Other measurements

Infrared spectra were obtained as Nujol mulls pressed between KBr windows, or in NaCl solution cells, between 400 and 4 000 cm^{-1} using a Perkin-Elmer Paragon 1000 spectrophotometer, UV/visible spectra with a Perkin-Elmer Lambda 12 spectrophotometer operating between 1 100 and 200 nm, in 1 cm quartz cells, NMR spectra were run on a Bruker DPX250 spectrometer, operating at 250.1 (^1H) and 62.9 MHz (^{13}C), and electron impact and positive ion fast atom bombardment mass spectra on a Kratos MS50 spectrometer, the FAB spectra employing a 3-nitrobenzyl alcohol matrix. CHN Microanalyses were performed by the University of Cambridge Department of Chemistry microanalytical service. Melting points are uncorrected. The EPR spectra for complexes **1**, **2**, **4** and **5** were obtained using a Bruker ESP300E spectrometer, fitted with the following attachments: at X band, an ER4102ST resonator and ER4111VT cryostat; and at Q band, an ER5106QT resonator and ER4118VT cryostat. Spectral simulations were performed using in-house software which has been described elsewhere.[42] X-Band EPR spectra of **3** were obtained using a Bruker ER200D spectrometer.

All electrochemical measurements were carried out using an Autolab PGSTAT20 voltammetric analyser, in MeCN or CH_2Cl_2 containing 0.1 or 0.5 M $NBu^n_4PF_6$ (prepared from NBu^n_4OH and HPF_6), respectively, as supporting electrolyte. Cyclic voltammetric experiments involved the use of a double platinum working/counter electrode and a silver wire reference electrode; all potentials quoted are referenced to an internal

Table 4 Experimental details for the single crystal structure determinations

	$[Cu(L^1)(Tp^{Ph})]\cdot CH_2Cl_2$ **1**·CH_2Cl_2	$[Cu(L^4Me)(Tp^{Ph})]\cdot CH_2Cl_2$ **4**·CH_2Cl_2	$[Cu(L^4Ph)(Tp^{Ph})]$ **5**
Formula	$C_{36}H_{31}BCl_2CuN_6O_2$	$C_{37}H_{34}BCl_2CuN_7O$	$C_{41}H_{34}BCuN_7O$
M_r	724.92	737.96	715.10
Crystal class	Triclinic	Triclinic	Monoclinic
Space group	$P\bar{1}$	$P\bar{1}$	$P2_1/n$
a/Å	12.828(3)	12.203(3)	12.680(2)
b/Å	13.962(7)	13.957(5)	18.890(3)
c/Å	9.859(3)	11.703(5)	15.5439(14)
α/°	94.71(3)	114.02(3)	—
β/°	90.39(2)	93.03(3)	110.412(12)
γ/°	81.77(3)	98.48(3)	—
U/Å^3	1741.7(11)	1786.6(11)	3489.4(8)
Z	2	2	4
μ(Mo-Kα)/mm^{-1}	0.822	0.801	0.670
T/K	293(2)	293(2)	173(2)
Measured reflections	5745	7876	7514
Independent reflections	5467	6281	6149
R_{int}	0.0742	0.0368	0.0413
$R(F)$	0.0735	0.0403	0.0483
$R'(F^2)$	0.2489	0.1103	0.1302
S	1.068	1.043	1.014

ferrocene–ferrocenium standard and were obtained at a scan rate of 100 mV s^{-1}. The number of electrons in a given voltammetric process was determined by comparison of the peak height with that of the $Fe^{II/III}$ couple shown by an equimolar amount of ferrocene. Spectroelectrochemical measurements were carried out using a Metrohm potentiostat connected to an optically transparent electrode system within a Perkin-Elmer Lambda 9 spectrophotometer.

EHMO Calculations were carried out using the CACAO package,[43] employing MM2-minimised molecular models.[44] The C–O single bond length was fixed at 1.362 Å for HL and at 1.260 Å for L$^{\bullet}$,[34,45] while the chalcogenoether substituents were constrained to be coplanar with the benzaldehyde ring.

Acknowledgements

The authors thank Dr Stuart Green (University of Leeds) for help with the calculations. The Royal Society (M. A. H.), the Government of Singapore (L. M. L. C.), the Committee of Vice-Chancellors and Principles (X. L.), the EPSRC, the University of Cambridge, the University of Leeds and the University of Edinburgh are acknowledged for financial support.

References

1 J. W. Whittaker, *Pure Appl. Chem.*, 1998, **70**, 903.
2 J. P. Klinman, *Chem. Rev.*, 1996, **96**, 2541.
3 M. M. Whittaker, P. J. Kersten, N. Nakamura, J. Sanders-Loehr, E. S. Schweizer and J. W. Whittaker, *J. Biol. Chem.*, 1996, **271**, 681.
4 N. Ito, S. E. V. Phillips, C. Stevens, Z. B. Ogel, M. J. McPherson, J. N. Keen, K. D. S. Yadav and P. F. Knowles, *Nature* (*London*), 1991, **350**, 87; N. Ito, S. E. V. Phillips, K. D. S. Yadav and P. F. Knowles, *J. Mol. Biol.*, 1994, **238**, 794.
5 A. J. Baron, C. Stevens, C. Wilmot, K. D. Seneviratne, V. Blakeley, D. M. Dooley, S. E. V. Phillips, P. F. Knowles and M. J. McPherson, *J. Biol. Chem.*, 1994, **269**, 25095.
6 M. M. Whittaker and J. W. Whittaker, *J. Biol. Chem.*, 1990, **265**, 9610.
7 J. M. Johnson, H. B. Halsall and W. R. Heineman, *Biochemistry*, 1985, **24**, 1579.
8 G. T. Babcock, M. K. El-Deeb, P. O. Sandusky, M. M. Whittaker and J. W. Whittaker, *J. Am. Chem. Soc.*, 1992, **114**, 3727.
9 R. Uma, R. Viswanathan, M. Palaniandavar and M. Lakshminarayanan, *J. Chem. Soc., Dalton Trans.*, 1994, 1219; H. Adams, N. A. Bailey, C. O. Rodriguez de Barbarin, D. E. Fenton and Q.-Y. He, *J. Chem. Soc., Dalton Trans.*, 1995, 2323; H. Adams, N. A. Bailey, I. K. Campbell, D. E. Fenton and Q.-Y. He, *J. Chem. Soc., Dalton Trans.*, 1996, 2233; M. Vaidyanathan, R. Viswanathan, M. Palaniandavar, T. Balasubramanian, P. Prabhaharan and T. P. Muthiath, *Inorg. Chem.*, 1998, **37**, 6418.
10 J. A. Halfen, V. G. Young, Jr. and W. B. Tolman, *Angew. Chem., Int. Ed. Engl.*, 1996, **35**, 1687.
11 J. A. Halfen, B. A. Jadzdzewski, S. Mahaptara, L. M. Berreau, E. C. Wilkinson, L. Que, Jr. and W. B. Tolman, *J. Am. Chem. Soc.*, 1997, **119**, 8217.
12 M. M. Whittaker, Y.-Y. Chuang and J. W. Whittaker, *J. Am. Chem. Soc.*, 1993, **115**, 10029; M. M. Whittaker, W. R. Duncan and J. W. Whittaker, *Inorg. Chem.*, 1996, **35**, 382.
13 Y. Wang and T. D. P. Stack, *J. Am. Chem. Soc.*, 1996, **118**, 13097; Y. Wang, J. L. DuBois, B. Hedman, K. O. Hodgson and T. D. P. Stack, *Science*, 1998, **279**, 537.
14 D. Zurita, C. Scheer, J.-L. Pierre and E. Saint-Aman, *J. Chem. Soc., Dalton Trans.*, 1996, 4331; D. Zurita, S. Ménage, J.-L. Pierre and E. Saint-Aman, *New J. Chem.*, 1997, **21**, 1001.
15 D. Zurita, I. Gautier-Luneau, S. Ménage, J.-L. Pierre and E. Saint-Aman, *J. Biol. Inorg. Chem.*, 1997, **2**, 46.
16 S. Itoh, S. Takayama, R. Arakawa, A. Furuta, M. Komatsu, A. Ishida, S. Takamuku and S. Fukuzumi, *Inorg. Chem.*, 1997, **36**, 1407.
17 A. Sokolowski, H. Leutbecher, T. Weyhermüller, R. Schnepf, E. Bothe, E. Bill, P. Hildenbrandt and K. Wieghardt, *J. Biol. Inorg. Chem.*, 1997, **2**, 444; J. Müller, T. Weyhermüller, E. Bill, P. Hildenbracht, L. Ould-Moussa, T. Glaser and K. Wieghardt, *Angew. Chem., Int. Ed.*, 1998, **37**, 616.
18 M. Ruf and C. G. Pierpont, *Angew. Chem., Int. Ed.*, 1998, **37**, 1736.
19 M. A. Halcrow, L. M. L. Chia, X. Liu, E. J. L. McInnes, L. J. Yellowlees, F. E. Mabbs and J. E. Davies, *Chem. Commun.*, 1998, 2465.
20 M. A. Halcrow, E. J. L. McInnes, F. E. Mabbs, I. J. Scowen, M. McPartlin, H. R. Powell and J. E. Davies, *J. Chem. Soc., Dalton Trans.*, 1997, 4025.
21 J. Perkinson, S. Brodie, K. Yoon, K. Mosny, P. J. Carroll, T. V. Morgan and S. J. Nieter Burgmayer, *Inorg. Chem.*, 1991, **30**, 719.
22 G. Casiraghi, G. Casnati, G. Pugli, G. Sartori and G. Terenghi, *J. Chem. Soc., Perkin Trans. 1*, 1980, 1862.
23 D. M. Eichhorn and W. H. Armstrong, *Inorg. Chem.*, 1990, **29**, 3607.
24 L. M. L. Chia, S. Radojevic, I. J. Scowen, M. McPartlin and M. A. Halcrow, to be published.
25 M. A. Halcrow, J. E. Davies and P. R. Raithby, *Polyhedron*, 1997, **16**, 1535.
26 See *e.g.* L. G. Hubert-Pfalzgraf and M. Tsunoda, *Polyhedron*, 1983, **2**, 203; D. C. Bradley, M. B. Hursthouse, J. Newton and N. P. C. Walker, *J. Chem. Soc., Chem. Commun.*, 1984, 188; F. A. Cotton, Z. Dori, R. Llusar and W. Schwotzer, *Inorg. Chem.*, 1986, **25**, 3529; G. Backes-Dahmann and J. H. Enemark, *Inorg. Chem.*, 1987, **26**, 3960; D. L. Hughes, G. J. Leigh and D. G. Walker, *J. Chem. Soc., Dalton Trans.*, 1988, 1153; E. Kime-Hunt, K. Spartalian, M. DeRusha, C. M. Nunn and C. J. Carrano, *Inorg. Chem.*, 1989, **28**, 4392; N. Abbaidi, C. J. Jones and J. A. McCleverty, *Polyhedron*, 1989, **8**, 1033; M. M. Taqui Kahn, P. S. Roy, K. Venkatasubramanian and N. H. Kahn, *Inorg. Chim. Acta*, 1990, **176**, 49; D. Collison, D. R. Eardley, F. E. Mabbs, A. K. Powell and S. S.

Turner, *Inorg. Chem.*, 1993, **32**, 664; F. A. Jalón, A. Otero and A. Rodriguez, *J. Chem. Soc.*, *Dalton Trans.*, 1995, 1629.
27 C. A. Hunter and J. K. M. Sanders, *J. Am. Chem. Soc.*, 1990, **112**, 5525.
28 R. S. Downing and F. L. Urbach, *J. Am. Chem. Soc.*, 1969, **91**, 597; T. N. Waters and P. E. Wright, *J. Inorg. Nucl. Chem.*, 1971, **33**, 359.
29 B. A. Goodman and J. B. Raynor, *Adv. Inorg. Chem.*, 1970, **13**, 135.
30 J. L. Stickney, M. P. Soriaga, A. T. Hubbard and S. E. Anderson, *J. Electroanal. Chem. Interfacial Electrochem.*, 1981, **125**, 73.
31 See *e.g.* G. G. Lobbia, C. Pettinari, F. Marchetti, B. Bovio and P. Cecchi, *Polyhedron*, 1996, **15**, 881.
32 S. M. Carrier, C. E. Ruggiero, R. P. Houser and W. B. Tolman, *Inorg. Chem.*, 1993, **32**, 4889.
33 C. Mealli, C. S. Arcus, J. L. Wilkinson, T. J. Marks and J. A. Ibers, *J. Am. Chem. Soc.*, 1976, **98**, 711.
34 G. J. Gerden, B. F. Bellew, R. G. Griffin, D. J. Singel, C. A. Ekberg and J. W. Whittaker, *J. Phys. Chem.*, 1996, **100**, 16739.
35 G. T. Babcock, M. K. El-Deeb, P. O. Sandusky, M. M. Whittaker and J. W. Whittaker, *J. Am. Chem. Soc.*, 1992, **114**, 3727.
36 A. R. Forrester, J. M. Hay and R. H. Thomson, *Organic Chemistry of Stable Free Radicals*, Academic Press, London, 1968, ch. 7, pp. 281–341.
37 S. G. N. Roundhill, D. M. Roundhill, D. R. Bloomquist, C. Landee, R. D. Willett, D. M. Dooley and H. B. Gray, *Inorg. Chem.*, 1979, **18**, 831; N. Kitajima, K. Fujisawa and Y. Moro-oka, *J. Am. Chem. Soc.*, 1990, **112**, 3210; *Inorg. Chem.*, 1990, **29**, 357; N. Kitajima, K. Fujisawa,T. Koda, S. Hikichi and Y. Moro-oka, *J. Chem. Soc.*, *Chem. Commun.*, 1990, 1357; N. Kitajima, T. Koda, S. Hashimoto, T. Kitagawa and Y. Moro-oka, *J. Am. Chem. Soc.*, 1991, **113**, 5664; N. Kitajima, K. Fujisawa, C. Fujimoto, Y. Moro-oka, S. Hashimoto, T. Kitagawa, K. Toriumi, K. Tatsumi and A. Nakamura, *J. Am. Chem. Soc.*, 1992, **114**, 1277; M. Ruff, B. C. Noll, M. D. Groner, G. T. Yee and C. G. Pierpont, *Inorg. Chem.*, 1997, **36**, 4860.
38 M. L. McGlashen, D. D. Eads, T. G. Spiro and J. W. Whittaker, *J. Phys. Chem.*, 1995, **99**, 4918.
39 M. M. Whittaker and J. W. Whittaker, *J. Biol. Chem.*, 1988, **263**, 6074.
40 G. M. Sheldrick, SHELXTL Plus, PC version, Siemens Analytical Instruments Inc., Madison, WI, 1990.
41 G. M. Sheldrick, SHELXL 93, University of Göttingen, 1993.
42 F. E. Mabbs and D. Collison, *Electron Paramagnetic Resonance of d Transition Metal Compounds*, Elsevier, Amsterdam, 1992, ch. 7.
43 C. Mealli and D. M. Proserpio, *J. Chem. Educ.*, 1990, **67**, 399.
44 CS CHEM3D Pro v. 3.5.1, Cambridge Soft Corporation, Cambridge, MA, 1997.
45 Y. Qin and R. A. Wheeler, *J. Am. Chem. Soc.*, 1995, **117**, 6083.

Paper 9/00741E